

Article

Dual-Polarized Dipole Antenna for Wireless Data and Microwave Power Transfer

Liangbing Liao, Zhiyi Li, Yuzhu Tang and Xing Chen *

College of Electronic and Information Engineering, Sichuan University, Chengdu 610064, China; liaoliangbing@126.com (L.L.); lizhiyi20212@163.com (Z.L.); tangyuzhu2020@163.com (Y.T.)

* Correspondence: chenxing@scu.edu.cn

Abstract: This manuscript presents a broadband high-efficiency dual-polarized dipole antenna for wireless power and data transfer. The proposed antenna mainly consists of cross-dipole patches, matching baluns, and a ground plane. The dual-polarized radiation mode was achieved by using two linear-polarization matching baluns to feed the cross-dipole patches orthogonally. The proposed dual-polarized dipole antenna realizes a bandwidth with S_{11} less than -10 dB (4.28 GHz–5.92 GHz) and a high radiation efficiency of about 95%. An independent rectifying circuit was designed, and a microwave energy transmission experiment was carried out. The final measured conversion efficiency for the two polarized ports at 5.8 GHz was about 77.6% and 76.4%, respectively. Simulation and measurement results showed that the proposed antenna is suitable for both wireless power and wireless data transfer applications.

Keywords: dual-polarized antenna; wideband; wireless power transfer



Citation: Liao, L.; Li, Z.; Tang, Y.; Chen, X. Dual-Polarized Dipole Antenna for Wireless Data and Microwave Power Transfer. *Electronics* **2022**, *11*, 778. <https://doi.org/10.3390/electronics11050778>

Academic Editor: Reza K. Amineh

Received: 9 January 2022

Accepted: 24 February 2022

Published: 3 March 2022

Publisher's Note: MDPI stays neutral with regard to jurisdictional claims in published maps and institutional affiliations.



Copyright: © 2022 by the authors. Licensee MDPI, Basel, Switzerland. This article is an open access article distributed under the terms and conditions of the Creative Commons Attribution (CC BY) license (<https://creativecommons.org/licenses/by/4.0/>).

1. Introduction

Currently, wireless power transmission is a research hotspot in the field of an intelligent Internet of Things (IoT), because microwave wireless energy transmission can transmit power to electronic systems or devices, particularly in some special scenarios where electrical energy cannot be provided via cables [1–4]. Wireless energy transmission has many potential applications. For example, a heart patient's pacemaker needs to be removed and replaced with a new pacemaker after the battery is depleted [5]. However, the battery can be charged by wireless energy transmission, to extend the service cycle of the battery. Another potential application is the wireless charging of drones in flight. Current UAVs carry a relatively limited battery energy in order to reduce the weight, which greatly limits the flight time and distance. However, through wireless energy transmission, it is possible to charge the flying drones in real time, thus extending the flight time [6].

To date, there have been many achievements in research into wireless energy transmission systems, mainly focusing on the problem of how to enhance the rectifying efficiency of wireless power transmission. In order to achieve high-efficiency wireless energy transmission, it is necessary to improve the radiation efficiency of the antenna, and also to improve the conversion efficiency of the rectifying circuit. Finally, impedance matching between the antenna and the rectifying circuit is needed, to achieve high transmission efficiency in the wireless energy transmission system. In the existing literature, some related studies have been conducted on improving the antenna radiation efficiency, to enhance the energy transmission efficiency. In [6], a linear-polarization-insensitive rectenna is proposed, which is suitable for ground-to-air wireless power transfer. The authors used a hybrid coupler to feed the dual-polarized aperture-coupled antenna, thus enabling the antenna to receive the horizontally polarized and vertically polarized components simultaneously. In [7], a radial line slot antenna is used to design a rectenna; this is the first time an eight-port circular sector subarray rectenna has been proposed. In [8], an adaptive reconfigurable rectenna is proposed, with a scheme realizing control of the states of the PIN switch by using the

rectifying voltage, which is a promising method for enhancing the rectenna integration and conversion efficiency. In [9], a pattern reconfigurable rectenna with switching omnidirectional and wide-beam patterns is presented, where the authors use a PIN switch to control the radiation modes. As the rectenna has a versatile structure, this can be applied to several transmitting antennas, in conformity with the direction of the incoming waves. In [10,11], polarized reconfigurable rectennas are proposed. In [12], a dual-polarized rectenna working at 2.45 GHz is presented, where a defected ground structure is used for harmonic rejection, but it has narrow bandwidth due to its slot feeding topology. A dipole antenna is commonly used as a rectenna due to its high radiation efficiency, stable pattern, and wide impedance bandwidth [13–16]. At present, the degree of integration of electronic communication systems is increasing more and more, as well as the requirement for multi-functionality. Therefore, in recent years, the function of the rectifier antenna system has no longer been independent. That is to say, the rectifier antenna system not only has the wireless energy transmission function but also requires the wireless data transmission function [17,18].

This manuscript presents a broadband high-efficiency dual-polarized dipole antenna, which consists of cross-dipole patches, matching baluns, and a ground plane. The dual-polarized radiation mode was realized by using two linear-polarization matching baluns to feed the cross-dipole patches orthogonally, and a wide impedance bandwidth was achieved by optimizing the matching balun and the cross-dipole patches. To verify its performance, an independent rectifying circuit was designed, and a microwave energy transmission experiment was carried out. The measured conversion efficiency for the two polarized ports at 5.8 GHz was 77.6% and 76.4%, respectively. Simulated and measured results demonstrated that the proposed antenna is suitable for both wireless energy transmission and wireless data transmission systems.

2. Rectenna Design

Antenna Structure

Figure 1 shows the design model of the proposed dual-polarized dipole antenna. As can be seen, the dipole antenna consists of an antenna ground plane, a pair of matching baluns, and a pair of cross-dipole patches. The antenna ground plane is printed on FR4 dielectric substrate with dielectric constant of 4.5, and the top surface of the antenna ground plane is printed with copper. The two matching baluns are installed vertically, and each matching balun contains a $\lambda/4$ wavelength feeding line, an open-circuit matching stub and a balun coupling microstrip. By properly designing the open-circuit matching stub size, broadband impedance matching can be achieved.

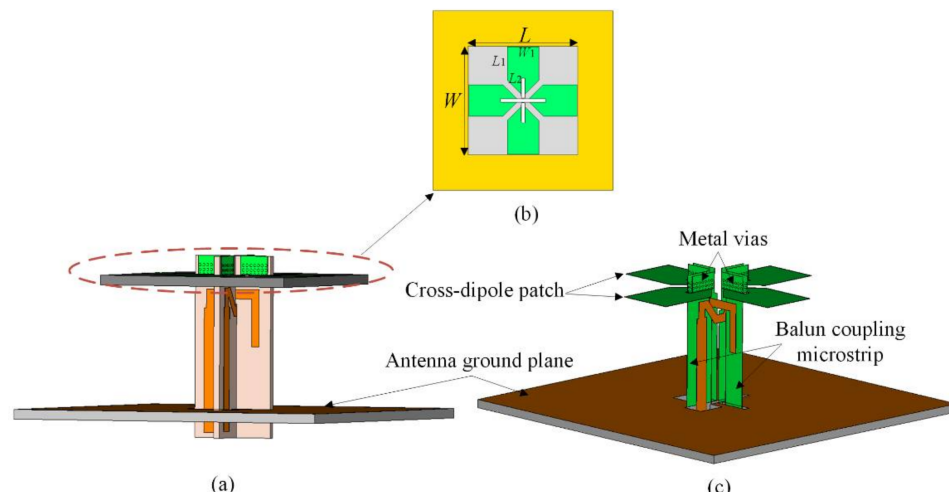


Figure 1. (a) Side view with dielectric substrate of matching balun and cross-dipole patches. (b) Top view of the cross-dipole patches. (c) Three-dimensional view without dielectric substrate of matching balun and cross-dipole patches.

In addition, by drilling two holes in the antenna ground plane, the matching balun can be plugged into the back of the antenna ground plane. When installed, the antenna ground plane and the balun coupling microstrips are electrically connected, but the $\lambda/4$ wavelength feeding lines are insulated from the antenna ground plane. The purpose of the antenna ground plane is to reflect the energy of the cross-dipole patches back and strengthen the directional performance, which is also appropriately optimized. It can be seen that the top of the balun coupling microstrip is connected to the cross-dipole patches. Multiple rows of metal vias are used to strengthen the electrical connection, which also help to facilitate welding and maintain reliable electrical contact.

To clearly show the structure of each polarized element, the disassembled model of the proposed antenna is shown in Figure 2. For a better description, the dual-polarized antenna can be divided into two elements, namely, polarized element 1 and polarized element 2. The biggest difference between the two polarized elements is the matching balun. Figure 2a–f shows the structure of polarized element 1 and polarized element 2, respectively. For polarized element 1, the matching stub is an L-shaped stub. For polarized element 2, the matching stub is an M-shaped stub. The matching stubs are optimized simultaneously to obtain a common wide impedance bandwidth. As can be seen, the two polarized ports, port 1 and port 2 are placed orthogonally. The optimized parameters of the proposed dual-polarized dipole antenna are as follows: $L = 24.3$ mm, $W = 24.3$ mm, $H = 13$ mm, $W_1 = 7$ mm, $W_2 = 1.6$ mm, $W_3 = 1$ mm, $W_4 = 1.6$ mm, $W_5 = 1$ mm, $L_1 = 7.5$ mm, $L_2 = 4.36$ mm, $L_3 = 11$ mm, $L_4 = 7$ mm, $L_5 = 5$ mm, $L_6 = 13$ mm, $L_7 = 2$ mm, $L_8 = 1.5$ mm, $L_9 = 2.5$ mm, $L_{10} = 1.8$ mm, and $L_{11} = 4$ mm.

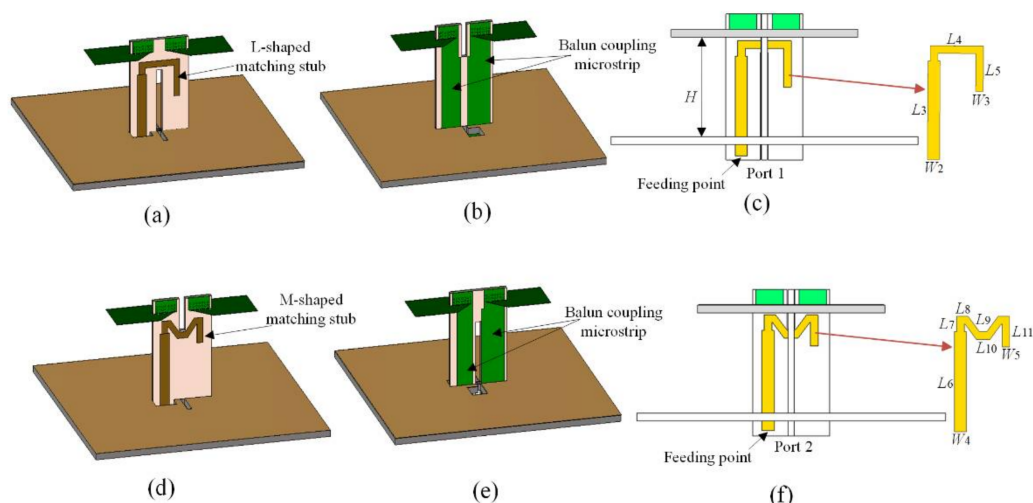


Figure 2. (a–c) Structure model of polarized element 1. (d–f) Structure model of polarized element 2.

The proposed antenna was modeled and simulated using the electromagnetic simulation software CST Studio Suite (2018). The simulated 3D radiation patterns of the two polarized ports are shown in Figure 3. It can be seen that unidirectional and wide beam properties are obtained, and the patterns are orthogonal since the two ports are excited by orthogonal polarization. Figure 4 shows the simulated radiation efficiencies for the two ports. The average radiation efficiency of the ports was about 95.5%.

The proposed antenna was fabricated to verify the actual antenna properties. Figure 5 shows photos of the fabricated antenna. The cross-dipole patches were printed on the FR4 substrate with dielectric constant of 4.5 and a thickness of 1 mm. The matching baluns were printed on Rogers RO4003C (Rogers, CT, USA) with a dielectric constant of 3.55 and a thickness of 0.813 mm. The tops of the baluns were welded to ensure a good and reliable electrical connection. Figure 6 shows the simulated and measured VSWR (Voltage Standing Wave Ratio). As can be seen, the measured common impedance wideband with $VSWR \leq 2$ covers a range of 4.28–5.92 GHz, which includes the 5.8 GHz microwave energy transmission band and the WLAN wireless data transmission band.

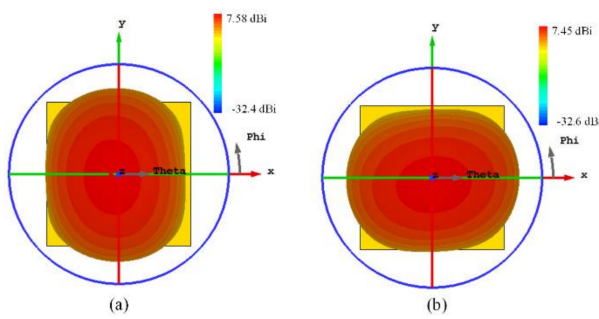


Figure 3. Simulated patterns at 5.8 GHz. (a) Port 1. (b) Port 2.

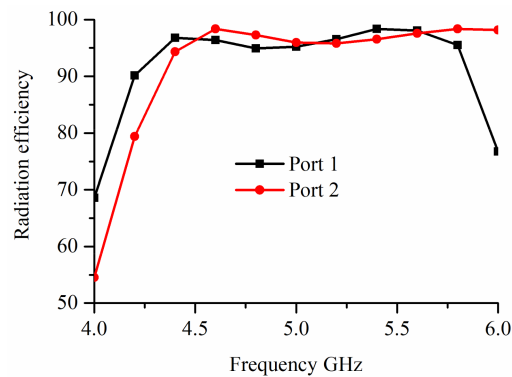


Figure 4. Simulated radiation efficiencies.

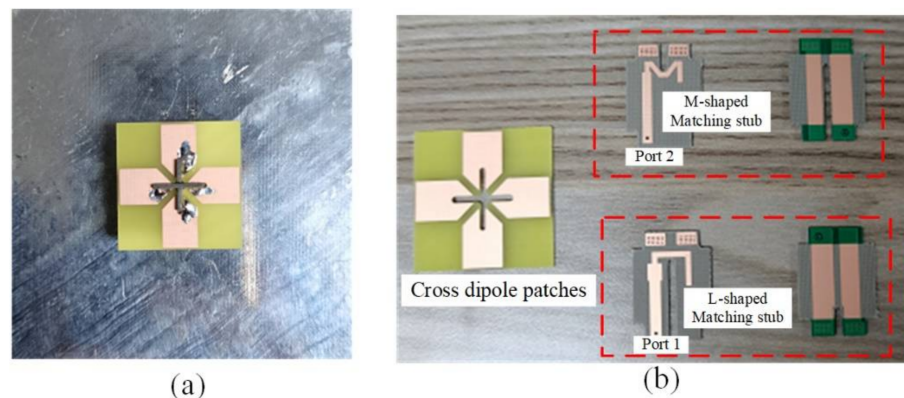


Figure 5. Fabricated antenna. (a) Top view. (b) Disassembled parts of the antenna.

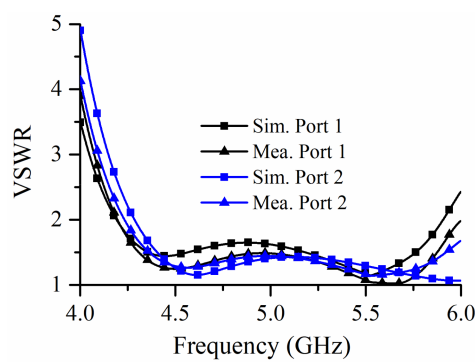


Figure 6. Simulated and measured VSWR.

Figure 7 shows the measured radiation efficiencies and gains of the two polarized elements. The radiation efficiencies and patterns were measured in an anechoic chamber. The average measured efficiency of the two ports was about 87.3% at the operating band,

and the average measured gain of the two ports was about 7.3 dBi. The radiation efficiencies and gains were flat within the working bandwidth, which shows a stable radiation performance. The decrease in antenna efficiency may be due to the loss of the RF connector and cables. Figures 8 and 9 present the measured 2D radiation patterns of the proposed antenna at 4.5 GHz, 5 GHz, and 5.5 GHz. Regardless of the orthogonal placement of the two polarized elements, their radiation patterns are similar across the whole operating band. For port 1, the 3 dB bandwidth at $\phi = 0^\circ$ (90°) was about 66° (90°). For port 2, the 3 dB bandwidth at $\phi = 0^\circ$ (90°) was about 90° (66°). The cross-polarization level was larger than 18 dB across the whole band.

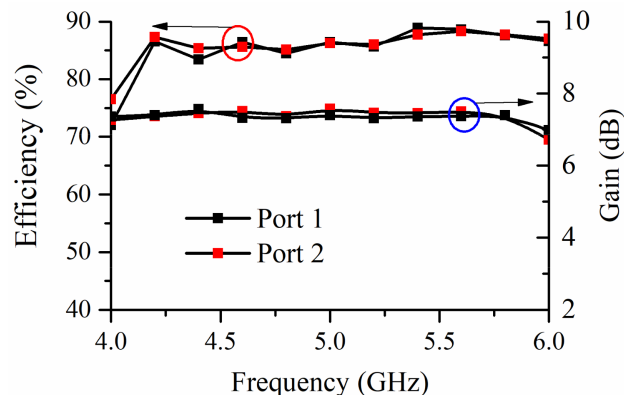


Figure 7. Measured radiation efficiencies and gains.

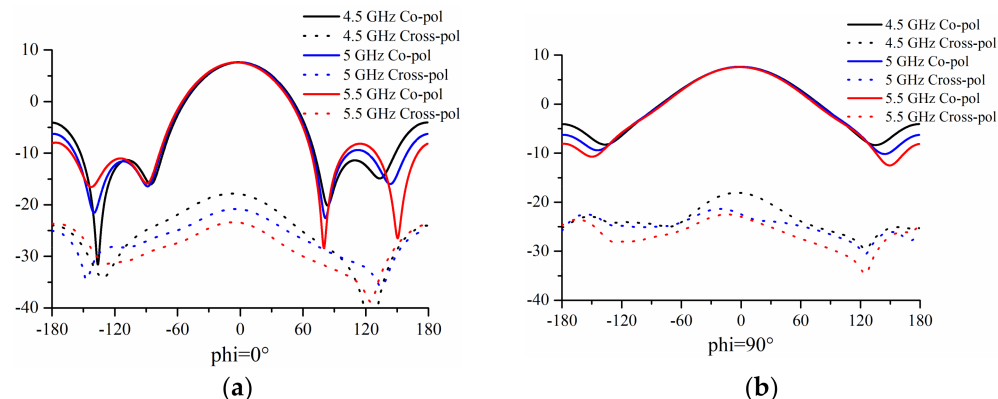


Figure 8. Measured 2D radiation patterns of Port 1: (a) at $\phi = 0^\circ$; (b) at $\phi = 90^\circ$.

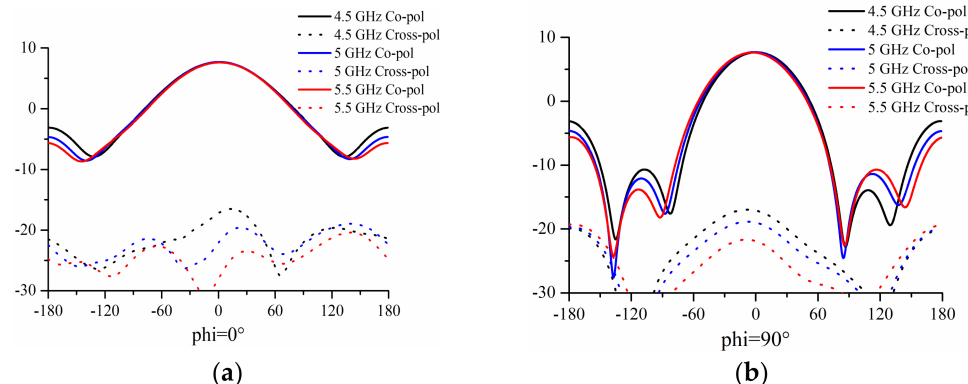


Figure 9. Measured 2D radiation patterns of Port 2: (a) at $\phi = 0^\circ$; (b) at $\phi = 90^\circ$.

3. Rectenna Measured Results

The schematic and the layout of the proposed rectifying circuit are shown in Figures 10 and 11, respectively. The detailed parameters of the rectifying circuit are exhibited in Figure 10, with parameter w_1 set to 1.6 mm, which is optimized for final impedance matching. As can be seen, the rectifying circuit consists of a T-shaped matching network, a pre-capacitor C_1 (100 pF), a bypass capacitor C_2 (100 pF), a rectifying diode HSMS-286F (Avago Technologies, San Jose, CA, USA), an output filter, and an adjustable load. The pre-capacitor C_1 can block the reversed DC current, and the bypass capacitor C_2 is able to suppress the high-order harmonics. An output filter is also used for suppressing the high-order harmonics. To facilitate debugging, we used a tunable resistance to act as the load R_{load} . The proposed rectifying circuit was printed on the bottom surface of the antenna ground plane. Each rectifying circuit was connected to a polarized antenna element.

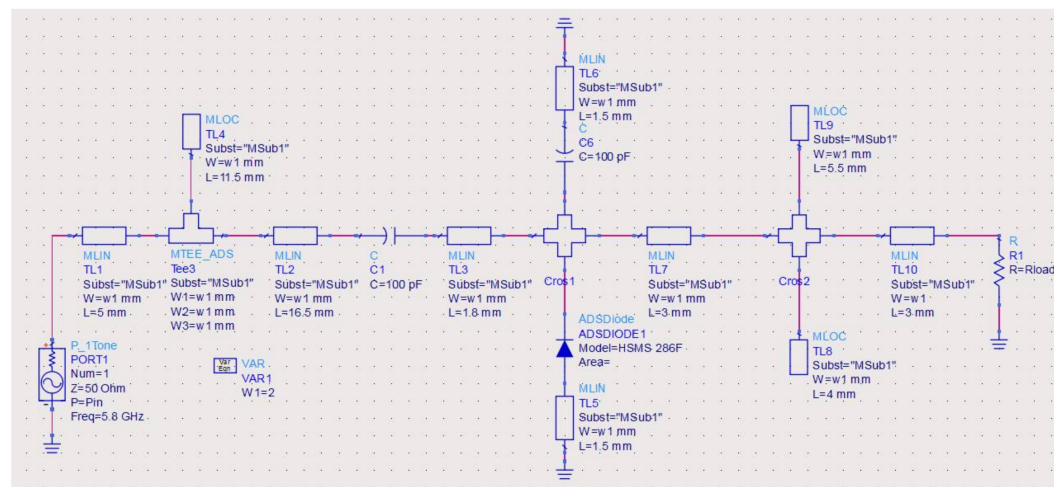


Figure 10. Schematic of rectifying circuit.

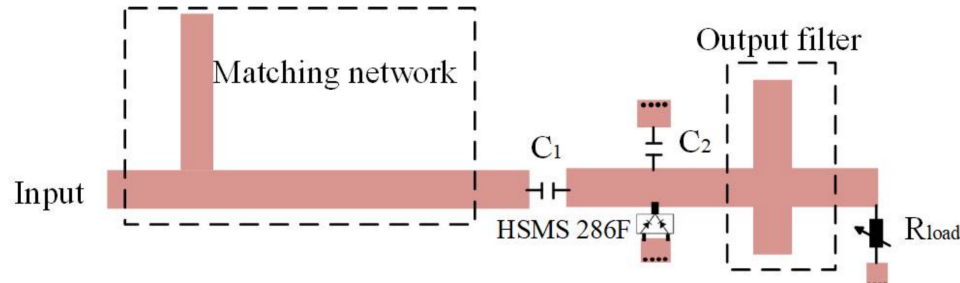


Figure 11. Layout of the fabricated rectifying circuit.

The output voltage of the rectifying circuit vs. the input power at 5.8 GHz is given in Figure 12, with the load R_{load} adjusted to 350 Ω . As the input power increases, the output voltage also increases. The fabricated antenna and rectifying circuit are shown in Figure 13a,b, and the wireless power transmission experiment was performed in an open environment surrounded by several absorbing materials, as shown in Figure 13c. To reduce the effect of the ground reflection, the absorbing materials were spread on the ground. During the experiment, a 10 dBi standard gain horn antenna was used for transmitting power. The horn and the antenna were set at the same height, and a voltmeter was used to detect the output DC voltage. The distance between the horn and the rectenna was 1 m, and the test frequency was 5.8 GHz. The load resistance R_{Load} was adjusted from 300 Ω to 400 Ω .

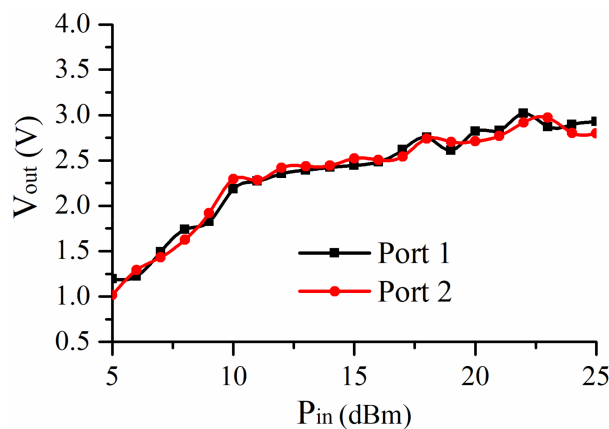


Figure 12. Output voltage vs. input power.

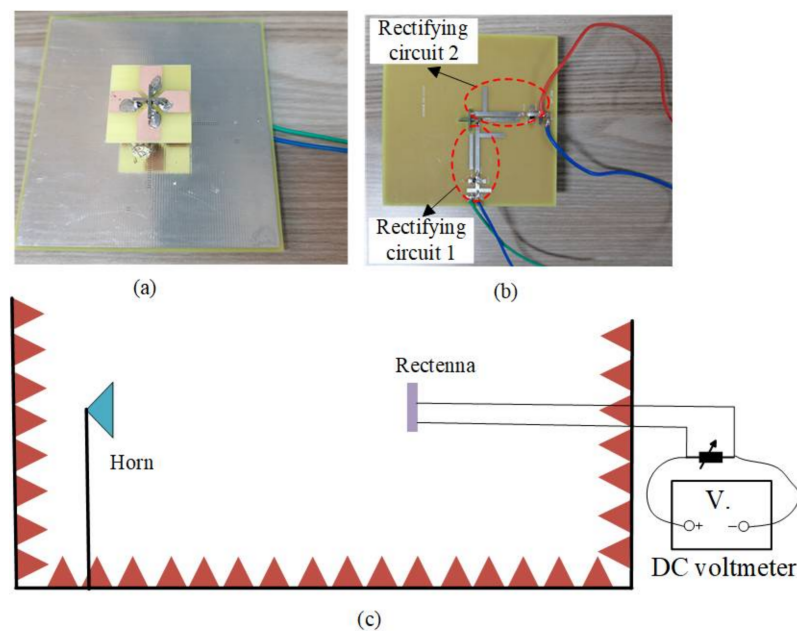


Figure 13. Photos of the proposed rectenna and the test setup. (a) Top view of the rectenna. (b) Back view of the rectenna. (c) Test environment.

The RF–DC conversion efficiency η_c can be calculated as

$$\eta_c = \frac{V_{Load}^2}{P_{in} R_{Load}} \quad (1)$$

where V_{load} is the DC voltage of the load R_{Load} , and P_{in} is the input power for the rectifying circuit. According to the far-field Friis transmission equation, the input power P_a of the rectenna can be expressed as

$$P_a = \frac{P_t G_t G_r \lambda^2}{(4\pi)^2 R^2} \quad (2)$$

where P_t is the source transmitting power, G_t is the gain of transmitting antenna, λ is the operating wavelength, and R represents the distance between the transmitting antenna and the rectenna.

$$P_{in} = P_a \eta_a \quad (3)$$

The test rectenna conversion efficiencies for the two polarized ports are shown in Figures 14 and 15, respectively. For port 1, when P_{in} was 18 dBm and R_{Load} was 385 Ω , the maximum measured conversion efficiency was 77.6% at 5.8 GHz. For port 2, when P_{in} was

15 dBm and R_{Load} was $365\ \Omega$, the maximum measured conversion efficiency was 76.4% at 5.8 GHz.

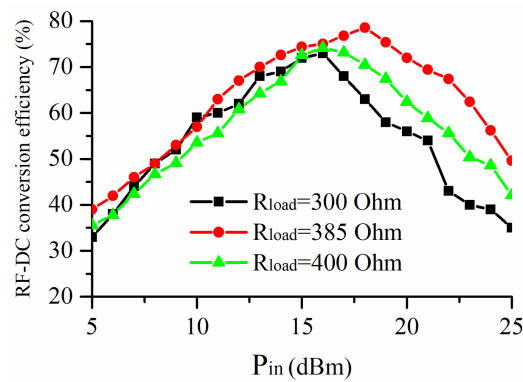


Figure 14. Measured RF-DC conversion efficiency under different loads R_{load} and input power values P_{in} , at port 1.

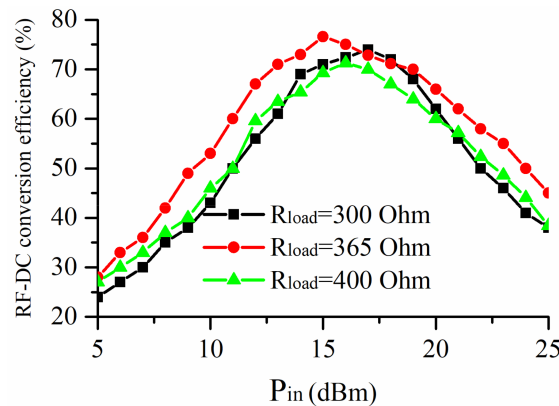


Figure 15. Measured RF-DC conversion efficiency under different loads R_{load} and input power values P_{in} , at port 2.

A comparison is shown in Table 1, between this study and the existing literature [2,3,12,15,16]. Our design has the characteristics of wide bandwidth and high efficiency, which makes it a candidate for current microwave wireless power transmission. Furthermore, the proposed antenna can easily be used to form a high-gain dual-polarized array, and hence it is also a candidate for simultaneous wireless data transmission.

Table 1. Comparison of the rectennas.

Ref.	Rectenna Bandwidth	Max. Eff.	Input Power
[2]	Narrow band (2.5 GHz)	78.7% (2.59 GHz)	25.6 dBm
[3]	Narrowband (2.4 GHz)	75% (2.4 GHz)	2 dBm
[12]	Narrowband (2.4 GHz)	83.7% (2.45 GHz)	22.5 dBm
[15]	Wideband (1.8–2.5 GHz)	70% (Not mentioned)	–10 dBm
[16]	Narrowband (2.45 GHz)	74.76% (2.45 GHz)	106.2 μ W/cm ²
This work	Wideband (4.28–5.92 GHz)	77.6% (5.8 GHz)	18 dBm

4. Conclusions

This paper presents a broadband high-efficiency dual-polarized dipole antenna, which consists of cross-dipole patches, matching baluns, and a ground plane. The dual-polarized radiation mode was realized using two linear-polarization matching baluns to feed the cross-dipole patches orthogonally, and wide impedance bandwidth was achieved by optimizing

the matching balun and the cross-dipole patches. To verify its performance, an independent rectifying circuit was proposed, and a microwave energy transmission experiment was carried out. The measured conversion efficiencies for the two polarized ports at 5.8 GHz were 77.6% and 76.4%. Simulated and measured results demonstrated that the proposed antenna is suitable for both wireless energy transmission and wireless data transmission systems.

Author Contributions: Conceptualization, L.L. and X.C.; validation, Y.T.; investigation, Z.L.; writing—original draft preparation, L.L.; writing—review and editing, X.C. All authors have read and agreed to the published version of the manuscript.

Funding: This work was partially supported by the National Natural Science Foundation of China (U19A2054).

Institutional Review Board Statement: Not applicable.

Informed Consent Statement: Not applicable.

Data Availability Statement: Not applicable.

Conflicts of Interest: The authors declare no conflict of interest.

References

- Li, X.; Yang, L.; Huang, L. Novel design of 2.45-GHz rectenna element and array for wireless power transmission. *IEEE Access* **2019**, *7*, 28356–28362. [[CrossRef](#)]
- Zhu, G.-L.; Du, J.-X.; Yang, X.-X.; Zhou, Y.-G.; Gao, S. Dual-Polarized communication rectenna array for simultaneous wireless information and power transmission. *IEEE Access* **2019**, *7*, 141978–141986. [[CrossRef](#)]
- Wagih, M.; Hilton, G.S.; Weddell, A.S.; Beeby, S. Weddell and Steve Beeby. Dual-polarized wearable antenna/rectenna for full-duplex and mimo simultaneous wireless information and power transfer (SWIPT). *IEEE Open J. Antennas Propag.* **2021**, *2*, 844–857. [[CrossRef](#)]
- Ding, S.; Koulouridis, S.; Pichon, L. Implantable wireless transmission rectenna system for biomedical wireless applications. *IEEE Access* **2020**, *8*, 195551–195558. [[CrossRef](#)]
- Asif, S.M.; Iftikhar, A.; Hansen, J.W.; Khan, M.S.; Ewert, D.L.; Braaten, B.D. A novel RF-power wireless pacing via a rectenna based pacemaker and a wearable transmit-antenna array. *IEEE Access* **2019**, *7*, 1139–1148. [[CrossRef](#)]
- Zhang, H.; Ngo, T. Linear-polarization-insensitive rectenna design for ground-to-air microwave power transmission. *IEEE Access* **2020**, *8*, 101702–101707. [[CrossRef](#)]
- Tomura, T.; Hirokawa, J.; Furukawa, M.; Fujiwara, T.; Shinohara, N. Eight-port feed radial line slot antenna for wireless power transmission. *IEEE Open J. Antennas Propag.* **2021**, *2*, 170–180. [[CrossRef](#)]
- Lu, P.; Song, C.; Cheng, F.; Zhang, B.; Huang, K. A self-biased adaptive reconfigurable rectenna for microwave power transmission. *IEEE Trans. Antennas Propag.* **2020**, *35*, 7749–7754. [[CrossRef](#)]
- Lu, P.; Yang, X.-S. Pattern reconfigurable rectenna with omni-directional/directional radiation modes for MPT with multiple transmitting antennas. *IEEE Microw. Wirel. Compon. Lett.* **2019**, *29*, 826–829. [[CrossRef](#)]
- Lu, P.; Yang, X.-S.; Li, J.-L.; Wang, B.-Z. Polarization reconfigurable broadband rectenna with tunable matching network for microwave power transmission. *IEEE Trans. Antennas Propag.* **2016**, *63*, 1136–1141. [[CrossRef](#)]
- Lu, P.; Song, C.; Huang, K.M. A two-port multipolarization rectenna with orthogonal hybrid coupler for simultaneous wireless information and power transfer (SWIPT). In *IEEE Transactions on Antennas and Propagation*; IEEE: Piscataway, NJ, USA, 2020.
- Lou, X.; Yang, G. A dual linearly polarized rectenna using defected ground structure for wireless power transmission. *IEEE Microw. Wirel. Compon. Lett.* **2018**, *28*, 828–830. [[CrossRef](#)]
- Tu, W.; Hsu, S.-H.; Chang, K. Compact 5.8 GHz rectenna using steeped-impedance dipole antenna. *IEEE Antennas Wirel. Propag. Lett.* **2007**, *6*, 282–284. [[CrossRef](#)]
- Niotaki, K.; Kim, S.; Jeong, S.; Collado, A.; Georgiadis, A.; Tentzeris, M.M. A compact dual-band rectenna using slot-loaded dual band folded dipole antenna. *IEEE Antennas Wirel. Propag. Lett.* **2013**, *12*, 1634–1637. [[CrossRef](#)]
- Song, C.; Huang, Y.; Zhou, J.; Zhang, J.; Yuan, S.; Carter, P. A high-efficiency broadband rectenna for ambient wireless energy harvesting. *IEEE Trans. Antennas Propag.* **2015**, *63*, 3486–34955. [[CrossRef](#)]
- Ou, J.-H.; Pan, J.; Dong, S.-W.; Zhang, X.Y. A dual-polarized rectenna with high efficiency at low input power density. In Proceedings of the 2020 14th European Conference on Antennas and Propagation (EuCAP), Copenhagen, Denmark, 15–20 March 2020.
- Lin, W.; Ziolkowski, R. Electrically small Huygens antenna-based fully-integrated wireless power transfer and communication system. *IEEE Access* **2019**, *7*, 39762–39769. [[CrossRef](#)]
- Zhang, Y.-M.; Li, J.-L. A dual-polarized antenna array with enhanced interport isolation for far-field wireless data and power transfer. *IEEE Trans. Veh. Technol.* **2018**, *67*, 10258–10267. [[CrossRef](#)]